THE SUN AS A LOW-FREQUENCY HARMONIC OSCILLATOR

P. E. DAMON and J. L. JIRIKOWIC

Laboratory of Isotope Geochemistry and The NSF-Arizona Accelerator Facility for Radioisotope Analysis, Department of Geosciences, The University of Arizona, Tucson, Arizona 85721 USA

ABSTRACT. Solar activity, as expressed by interplanetary solar wind magnetic field fluctuations, modulates the atmospheric production of ^{14}C. Variations of atmospheric ^{14}C can be precisely established from the cellulose within annual tree rings, an independently dated conservative archive of atmospheric carbon isotopes. $\Delta^{14}C$ time series interpretation shows that solar activity has varied with a recurrence period of 2115 ± 15 (95% confidence) yr (Hallstattzeit) (Damon & Sonett 1991) over the past 7160 yr. From a non-stationary oscillation solar activity hypothesis, 52 possible spectral harmonics may result from this period. Damon and Sonett (1991) identify powerful harmonics such as the 211.5-yr (Suess) and the 88.1-yr (Gleissberg) cycles as independent fundamental periods. These stronger harmonics appear to modulate the 11-yr (Schwabe) sunspot cycle. Variations in the solar magnetic field, thus, may respond to longer period variations of the solar diameter envelope (Ribes *et al.* 1989). Such variations would affect solar radiative energy output and, consequently, change total solar irradiance (Sofia 1984).

HARMONIC ANALYSIS OF THE ^{14}C SPECTRUM

Spectral analysis of the available high-precision $\Delta^{14}C$ data by Stuiver and Braziunas (1989), using the maximum entropy method (MEM), led them to postulate a fundamental 420-yr oscillation related to changes in the solar convective zone. After increasing the model autoregressive order (AR, equivalent to the length of the prediction error filter, for the purposes of this paper), Stuiver and Braziunas observed that additional periods became important. They note that the 420-yr period splits into periods of 504, 355 and 299 yr. We have observed that this apparent splitting of the 420-yr peak results from the limited frequency resolution, and to oversmoothing by the MEM spectral method when too small an AR order is chosen. Our experience suggests that frequency resolution for MEM (AR = 160) spectral analysis lies between $1/\tau$ and $1/1.25\tau$, where τ is the length of the time series. Although the analysis above seems to suggest subjectivity, MEM analyses provide excellent frequency resolution when comparing between many AR orders and with the results of alternative spectral estimate methods (such as the discrete Fourier transform (DFT), multi-taper estimates, maximum-likelihood-Bayesian methods and singularity spectral-analysis estimates). By varying the number of sampled points and AR order, it becomes apparent that the 420-yr peak does not split, but each of these peaks is always present with relative peak heights varying with chosen AR order.

However, these low-frequency variations remain poorly resolved, whatever the spectral method employed, until either the data time series lengthens, or a hypothesis develops relating the poorly resolved low-frequency variations to better-resolved higher-frequency variations (see Damon & Jirikowic 1992, for details). We have used the simplest non-stationary model, a harmonic oscillator, as our working hypothesis. The well-resolved higher-frequency variations represent a set of harmonic and combination overtones of lower-frequency variations. For example, concerning the ~504-yr period, its 2nd–13th apparent overtones observed in spectral analyses of the last 7160 yr of the high-precision bidecadal $\Delta^{14}C$ calibration time series (Stuiver & Kra 1986) establish the period more precisely as 526 yr. Similarly, the 9 apparent overtones of the 420-yr peak define it as 424 yr; the 8 apparent overtones of the 355-yr period establish it as 356 yr, and analysis of the 299-yr period with 6 apparent overtones established it more precisely at 300 yr. Further, each of these longer periods appears to modulate shorter periods producing peak triplets, quintets and higher. Further analyses show these spectral peak frequencies may be related as elements of the

harmonic series T/n, T/2n, T/3n, . . ., where n is any positive integer, 1, 2, 3, . . . Assuming n = 1, and finding an approximate least-common multiple to obtain the shortest possible estimated period of the fundamental, T, we obtained (keeping 4 significant figures to reduce truncation errors):

$$526 \times 4 = 2104$$
$$424 \times 5 = 2120$$
$$356 \times 6 = 2136$$
$$300 \times 7 = 2100$$
$$T = 2115 \pm 9 \text{ yr } (\bar{\sigma})$$

Thus, the supposed fundamentals may be harmonic overtones of a ~2115-yr Hallstattzeit period (Damon & Sonett 1991). By hypothesis that the Hallstattzeit period may have 52 harmonic overtones present in the spectral analyses (limited only by the 40-yr Nyquist period of the bidecadal $\Delta^{14}C$ time series), the fundamental period may be established from the observed peak power frequencies with a precision of 0.1 ± 3.1 yr (95% confidence level). The agreement of the Hallstattzeit overtones with reference to both the DFT and MEM (AR = 160) spectra (Fig. 1) strongly suggests that the causal phenomenon is independent of the spectral method. Thus, modulation side-lobe "leakage" due to spectral window truncation does not seem to influence greatly our results.

PROBABILISTIC VALIDATION OF THE HALLSTATTZEIT OVERTONES

The probabilistic[1] significance of this agreement may be investigated in several ways. For example, of the 20 DFT frequencies with spectral power > 95% χ^2-confidence, 7 have frequencies matching the hypothesized Hallstattzeit harmonic overtone frequencies within the frequency resolution.[2] From the discrete, multinomial distribution of these sets of frequencies, the probability of equaling the performance of the Hallstattzeit harmonic hypothesis with 52 randomly chosen frequencies is 0.12%. The likelihood of the harmonic hypothesis reaches a maximum near a fundamental period of 2115 yr, and remains above 95% from 2120 to 2105 yr. From Bayesian analysis, we are able to infer from the null hypothesis *a priori* probability distribution of random matching that the *a posteriori* probability of random matching remains zero within 95% confidence for hypothetical fundamental periods between 2130 and 2100 yr. The final test employed the second order norm between the observed spectral peak frequencies and the hypothesized overtone frequencies. A Hallstattzeit fundamental period of 2116-yr minimized the second order norm with a 2σ (~95%) range from 2128 to 2104 yr. Thus, the solar harmonic oscillator hypothesis with a fundamental Hallstattzeit period between 2130 and 2100 yr provides a compelling explanation of much of the observed $\Delta^{14}C$ time series spectrum.

MODULATION OF THE SOLAR SCHWABE CYCLE BY THE SUESS AND GLEISSBERG HARMONICS

A harmonic oscillator would be a particular solution to the general differential equation

$$\ddot{D}(t) + f[\dot{D}(t)] + g[D(t)] = F(t) \qquad (1)$$

[1]Because the hypothesized 2115-yr Hallstattzeit variation recurs only three times in the ^{14}C calibration time series, and the harmonic overtones may not have independent statistical distributions, non-parametric probability analyses may be more reliable and informative than traditional parametric statistics.

[2]At any given frequency, the MEM absolute power depends upon the chosen AR order. Thus, conventional confidence-level calculation analysis of MEM spectral peaks is inappropriate without independent *a priori* determination of the AR order.
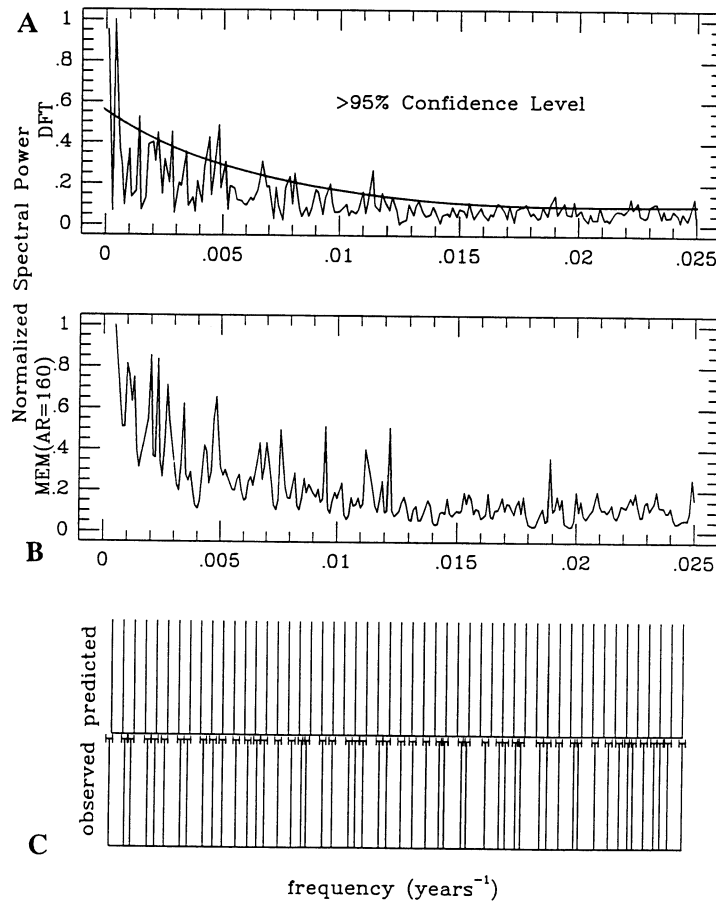
Fig. 1. A. DFT power spectrum of the high-precision $\Delta^{14}C$ data. Vertical lines represent the Hallstattzeit fundamental and 52 harmonic overtones. The heavy curve estimates the lower 95% χ^2-confidence limit and the "red-noise continuum" likely due to non-stationarity and time persistence. B. MEM (AR = 160) spectrum. Note that although much of the spectrum trends as a red-noise continuum, 20 spectral peaks extend above the 95% χ^2-confidence limit, suggesting substantial periodicity. C. compares the observed and predicted spectral peaks. The error bars on the top of the observed lines represent the frequency resolution.

where D(t) represents solar activity, f, a damping function, g, a restoring function and F(t), an external forcing. The harmonic oscillator particular solution of Equation (1) may take the form of a Fourier sum of harmonics

$$D(t) = A_0 + \sum_{i=1}^{n} [A_i\cos(\omega_i t-\phi_i)-B_i\sin(\omega_i t-\phi_i)] \qquad (2)$$

where ω_i are harmonic frequencies, A_i and B_i are amplitude coefficients and ϕ_i are phase coefficients. Note that A_i, B_i and ϕ_i may be complex functions of both the harmonic frequencies and time.

Certain harmonics of the Hallstattzeit with observed power greater than expected for a simple system of harmonics act as apparent fundamentals (*i.e.*, 211.5-yr Suess and 88.1-yr Gleissberg variations). These periods appear in the DFT and MEM (AR = 160) spectra of the annual Wolf sunspot indices as harmonic overtones and modulating periods (Fig. 2). For example, the first two
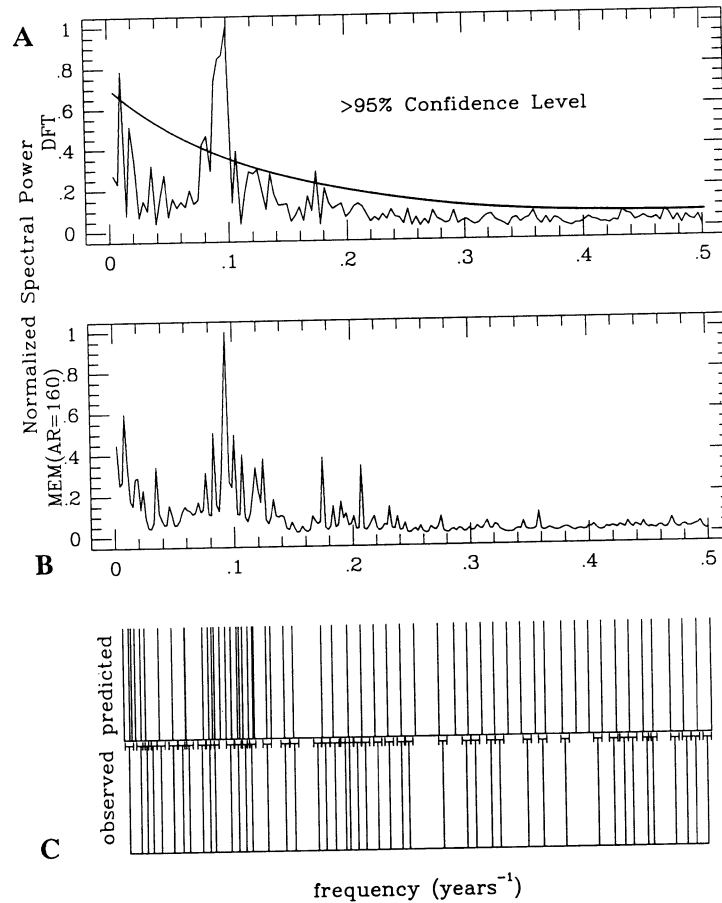
Fig. 2. A. DFT power spectrum of the annual Wolf sunspot index. Vertical lines represent the 211.5, 88.3 and 11.1-yr periods, their overtones and sidebands produced by amplitude modulation of the 11.1-yr carrier period (after Sonett 1982). The heavy curve estimates the lower 95% χ^2-confidence level and the red-noise continuum. B. MEM (AR = 160) spectrum. Vertical lines represent observed peaks. Modulation sidebands appear in the annual Wolf sunspot index spectra, features not seen in the $\Delta^{14}C$ spectra in Figure 1. C. compares the observed spectral peaks with those predicted from the amplitude modulation model of the 11-yr cycle. The error bars on the top of observed lines represent the frequency resolution.

harmonic overtones of the 211.5-yr Suess period cannot be resolved from the 88.1-yr Gleissberg period, and not all side bands of the 11.1-yr Schwabe cycle carrier modulated by these longer periods and their overtones can be resolved from one another (Fig. 2). Higher-frequency overtones appear, including four overtones of the 11.1-yr carrier (5.55, 3.70, 2.78 and 2.22-yr, see Fig. 2). The 211.5-yr period and its 2nd (105.8-yr) and 4th (52.9-yr) overtones, combined with the Gleissberg period (88.1-yr), appear to modulate strongly the 11.1-yr carrier. A reasonable fit to the observed annual Wolf sunspot indices can be obtained, using a squared amplitude modulation model (after Sonett 1982) by allowing these periods (211.5, 105.8, 52.9 and 88.1-yr) to amplitude modulate the 11.1-yr carrier signal (see Fig. 3, Table 1)

$$R_z = \sum_{i=1}^{4} \alpha_i \cos^2(\omega_i t + \phi_i) \alpha_c \cos^2(\omega_c t + \phi_c) \quad . \tag{3}$$
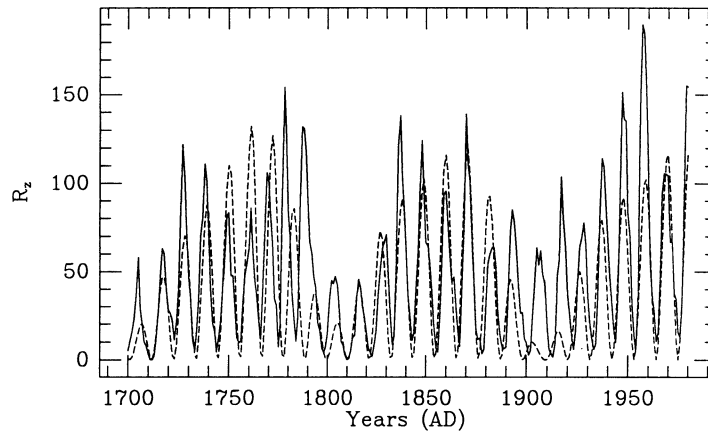
Fig. 3. (- - -) simulation of the (——) annual Wolf sunspot indices by modulation of the 11.1-yr carrier by the 211.5, 105.75, 88.125 and 52.875-yr periods with the amplitudes and phases shown in Table 1. Note that the 211.5-yr periodicity has a low modulation coefficient. Also note that the model underestimates sunspot indices during the late 19th century solar activity minimum. Because the Hallstattzeit gate strongly affects the 211.5-yr harmonic and this millennium's Hallstattzeit-gating epoch ends before the late 19th century, the weak 211.5-yr and the weak late 19th century solar minimum would support the Hallstattzeit non-stationarity hypothesis (see text for details).

TABLE 1. Model Parameters for Modulation of the 11.1-Year Schwabe Carrier

Index	Period	α	ϕ
1	52.875	0.66	0.62
2	88.125	0.43	−1.82
3	105.75	1.31	1.10
4	212.5	0.01	1.33
c	11.1	65.4	1.46

Note that the cosine series modulation function expressed in Equation 3 is a member of the family of harmonic oscillator solutions given in Equation 2. Notably, the model fits the late 19th century minimum poorly. Mean sunspot indices do not fall to the very low levels predicted by our model. Also note that the modulation coefficient, alpha, for the 211.5-yr period is quite small. Both events may be explained by the non-stationarity present in the Wolf sunspot index data set. The Hallstattzeit epoch encompassing the Wolf, Spörer, Maunder and Dalton solar activity minima wanes in the first half of the sunspot index data. Thus, the stationary model assumption has been compromised. The Hallstattzeit variation also appears to modulate strongly the 211.5-yr period (Damon & Sonett, 1991). A more sophisticated model would include the Hallstattzeit gating.

HALLSTATTZEIT GATING: PHYSICAL MANIFESTATION AND PALEOCLIMATIC CONSEQUENCES?

The Hallstattzeit variation appears.to act as a gate (Damon 1988) allowing more intense century-scale oscillation during the high $\Delta^{14}C$ phase of the cycle (*e.g.*, the Maunder and Hallstattzeit low solar activity epochs; Schmidt & Gruhle 1988). If we assume the wave form for the Hallstattzeit period, shown in Figure 4, with the high $\Delta^{14}C$ phases appearing as the square-wave gate portions, the square wave generates the harmonic overtones and strongly modulates the 211.5, 88.1-yr periods. Figure 4 presents the $\Delta^{14}C$ variations after the removal of a very long-term trend ascribed to changes in the Earth's magnetic dipole moment (see Damon & Sonett 1991 for review). The
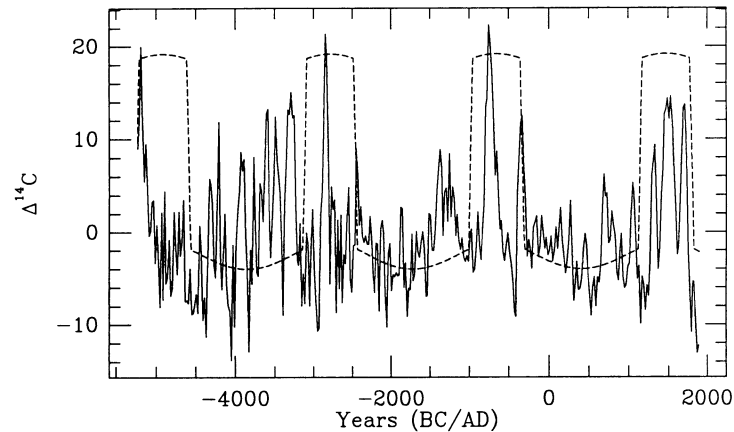
Fig. 4. (– – –) wave-form model generating the Hallstattzeit harmonics and amplitude gating of the (——) century-scale $\Delta^{14}C$ variations compared to the detrended high-precision $\Delta^{14}C$ time series. Note that the weaker century-scale oscillations appear modulated by variations of the Earth's magnetic field as described in the text, yet the stronger gated variations appear comparatively unmodulated.

trend can be closely fit by a sine curve with a 10,780-yr period for the last eight millennia, but deviates markedly during the early Holocene (Damon, Cheng & Linick 1989). The Earth's magnetic dipole moment is weak during the negative portion of this cycle before 2600 BC and stronger during the positive part of the cycle between 2600 BC and AD 1650. The effect of this geomagnetic field variation can be seen by relative suppression or enhancement of the century-scale $\Delta^{14}C$ variations. This amplitude modulation of $\Delta^{14}C$ variations by the geomagnetic field appears weak during the high $\Delta^{14}C$ gating portion of the Hallstattzeit cycle. The Hallstattzeit variation may have also affected paleoclimate by changing solar output and the Suess and Gleissberg cycles may have contributed in part to the global warming trend evidence since the last decade of the 19th century (Damon 1989; Damon & Jirikowic 1992; see Damon & Sonett 1991 for review).

The physical manifestation of the Hallstattzeit solar variation has yet to be conclusively determined. Ribes (1990: 96), reviewing the evidence for periodicities in the solar diameter, concludes that, "the Sun's apparent radius was larger in the deep of the Maunder Minimum (late in the Little Ice Age, when practically no sunspots were seen) than it was at the end when solar activity has resumed (from 1705 onwards). An expansion of solar envelope of about 3 arc seconds on the diameter would be consistent with cooling of the envelope and with a slowing down of surface rotation." With relation to Ribes' (1990) interpretation, the Hallstattzeit wave form in Figure 4 suggests that the Sun slowly expands, lingers at maximum diameter and then contracts. This structural modulation partitions potential energy and radiant energy (Sofia 1984) between two intransitive states.

CONCLUDING REMARKS

The harmonic overtone periods may represent a dynamic-system response and other non-stationary phenomena or a mathematical manifestation of the non-sinusoidal Hallstattzeit variation. The observation of variations, such as the ≈88-yr Gleissberg cycle, strongly suggests that several variations also have a physical reality beyond being harmonic overtones of the fundamental Hallstattzeit variation. Such secular solar variations would have obvious implications as possible factors in global climate change. Associating these Hallstattzeit solar variations with climate variations may require a time-variant climate model. Further, the apparent non-stationarity of the

solar variations prohibits extrapolating linear regression models calibrated over a single 11-yr cycle between solar activity and solar radiant output beyond a Hallstattzeit variation. Predictions based solely upon the cyclicity of $\Delta^{14}C$ variations, without consideration of these Hallstattzeit non-stationarities, may be more misleading than informative. Understanding both the modeling and geophysical implications of the Hallstattzeit variation would advance our ability to predict solar activity and understand the Sun as a harmonic oscillator.

ACKNOWLEDGMENTS

REFERENCES

Damon, P. E. 1988 Production and decay of radiocarbon and its modulation by geomagnetic field-solar activity changes with possible implications for the global environment. *In* Stephenson, F. R. and Wolfendale, A. W., eds., *Secular Solar and Geomagnetic Variations in the Last 10,000 Years*. Dordrecht, The Netherlands, Kluwer Academic Publishers: 267–286.

_____1989 Radiocarbon, solar activity and climate. *In* Avery, S. K. and Tinsley, B. A., eds., *Proceedings from the Workshop on Mechanisms for Tropospheric Effects of Solar Variability and the Quasi-Biennial Oscillation*: 198–208.

Damon, P. E., Cheng, S. and Linick, T. W. 1989 Fine and hyperfine structure in the spectrum of secular variations of atmospheric ^{14}C. *In* Long, A. and Kra, R. S., eds., Proceedings of the 13th International ^{14}C Conference. *Radiocarbon* 31(3): 704-718.

Damon, P. E. and Jirikowic, J. L. 1992 Radiocarbon evidence for low frequency solar oscillations. *In* Povinec, P., ed., *Rare Nuclear Processes, Proceedings of the 14th Europhysics Conference on Nuclear Physics*. Singapore, World Scientific Publishing Co.: 177-202.

Damon, P. E. and Sonett, C. P. 1991 Solar and terrestrial components of the atmospheric ^{14}C variance spectra. *In* Sonett, C. P., Giampapa, M. S. and

Matthews, M. S., eds., *The Sun in Time*. Tucson, The University of Arizona Press: 360–388.

Ribes, E. 1990 Astronomical determinations of the solar variability. *Philosophical Transactions of the Royal Society of London* A 330: 487–497.

Ribes, E., Merlin, P., Ribes, J. C. and Barthalot, R. 1989 Absolute periodicities of the solar diameter, derived from historical and modern time-series. *Annals Geofisica* 1: 321–329.

Schmidt, B. and Gruhle, W. 1988 Radiokohlenstoff-gehalt und dendrochronologie. *Naturwissenschaftliche Rundschau* 5: 177–182.

Sofia, S. 1984 Solar variation as a source of climate change. *In* Hansen, J. E. and Takahashi, T., eds., *Climate Processes and Climate Sensitivity*. Washington, American Geophysical Union: 202–206.

Sonett, C. P. 1982 Sunspot time series: Spectrum from square law modulation of the Hale Cycle. *Geophysical Research Letters* 9: 1313–1316.

Stuiver, M. and Braziunas, T. F. 1989 Atmospheric ^{14}C and century-scale solar oscillations. *Nature 338*: 405–408.

Stuiver, M. and Kra, R. S., eds. 1986 Calibration Issue. Proceedings of the 12th International ^{14}C Conference. *Radiocarbon* 28(2B): 805–1030.